HAIT Journal of Science and Engineering, Volume 1, Issue 1, pp. 51-64

Occurrence of non-Drude behavior in the infrared conductivity of ruthenates and cuprates

Smadar Shatz*, Lior Klein, and Nathan Wiser

Department of Physics, Bar-Ilan University,
Ramat-Gan 52900, Israel
* *Corresponding author: shatz@mail.biu.ac.il*
Received 5 December 2003

Abstract

The infrared conductivity $\sigma(\omega)$ of very-high-resistivity ruthenates and cuprates (in the normal state) was recently found to deviate from the usual Drude behavior - $\sigma_{\mathrm{Drude}}(\omega) \propto \omega^{-2}$. We have included the Pippard ineffectiveness condition in the analysis of $\sigma(\omega)$, and obtained that for very-high-resistivity materials, $\sigma(\omega) \propto \omega^{-\alpha}$, with $\alpha \ll 2$. Therefore, the Pippard condition might be a partial explanation for the non-Drude behavior observed for the infrared conductivity of the ruthenates and cuprates.

PACS: 72.10.-v, 72.30.+q, 74.72.-h

1 Introduction

An electronic property much studied experimentally [1 - 5] is the complex frequency-dependent conductivity $\sigma(\omega)$. As is well known [6] the Landau fermi-liquid theory (LFLT) predicts that the real part of the conductivity, $\sigma_1(\omega)$, follows the Drude law, which yields that for high (infrared) frequencies, $\sigma_{\mathrm{Drude}}(\omega) \propto \omega^{-2}$. The Drude law is obeyed for ordinary metals, both the non-superconductors (e.g., noble metals) as well as conventional superconductors (e.g., Al, Hg) above the critical temperature T_c. On the other hand, recent experiments show that the Drude law does not hold for very-high-resistivity materials, such as the ruthenates and the cuprates in the

normal state. For both the ruthenate [1, 2] $SrRuO_3$ and the cuprates (high-temperature superconductors in the normal state) [3, 4, 5] the infrared-frequency conductivity data yield $\sigma_1(\omega) \propto \omega^{-\alpha}$, with $\alpha \ll 2$.

The non-Drude behaviour for $\sigma_1(\omega)$ discussed here is particularly significant because it was observed for samples characterised by a high degree of crystallinity. This ensures that effects of disorder are not the cause of the observed non-Drude behaviour. For all the data that we discuss here, the experimentalists stressed the high quality of the measured samples: "grown epitaxially" [1 - 3] "distinguished by large residual resistivity ratios" [2] "crystallinity of the samples" [3, 5] etc. Correspondingly, the electron mean free path λ of such samples is very much longer than the lattice constant in the relevant temperature range. For example, Santi and Jarlborg [6] give the value $\lambda = 135$ Å for $SrRuO_3$.

In view of the crystallinity of the samples that were measured, these seemingly anomalous $\sigma_1(\omega)$ data have frequently been interpreted as evidence for the breakdown of the LFLT for these materials. However, we here suggest that there may be another cause that also contributes to these results for $\sigma_1(\omega)$. In particular, if one includes the Pippard ineffectiveness condition (to be explained later) in the analysis of $\sigma_1(\omega)$, then even within the framework of the LFLT, one obtains non-Drude behavior for very-high-resistivity materials.

We are not claiming that the ruthenates and cuprates are fermi-liquid materials. Rather, our goal here is to call attention to the fact that the optical conductivity can exhibit a richer variety of behaviour within the framework of fermi-liquid theory when the Pippard condition is included. Thus, the observed non-Drude behaviour for $\sigma_1(\omega)$ is not *by itself* sufficient evidence to establish the breakdown of the LFLT for high-resistivity materials.

In Section 2, we present the experimental data for $\sigma_1(\omega)$. The Pippard ineffectiveness condition is discussed in Section 3 and is generalized to include time-dependent fields in Section 4. In Section 5, a model is introduced for including the Pippard condition in the analysis of $\sigma_1(\omega)$, and the results are compared with experiment in Section 6. The summary follows in Section 7.

2 Experiment

2.1 Ruthenates

Dodge *et al.* [1] have discussed the temperature dependence of $\sigma_1(\omega)$ for $SrRuO_3$ over an unusually wide range of frequencies, based on data obtained by the experimental method appropriate to each range of ω. The data are displayed in Fig. 1 for four temperatures, ranging from 8 K to 80 K. (The curves will be discussed presently.) The experimental methods used include terahertz time-domain spectroscopy (squares) [1] far-infrared transmission (triangles) [1] and infrared reflectivity (circles) [2]. These workers found a consistent picture for $\sigma_1(\omega)$ over three decades of frequency, as shown in the figure.

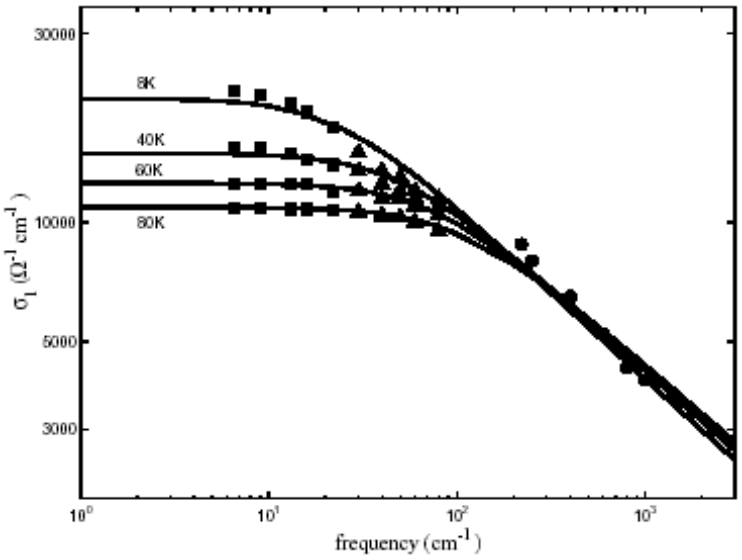

Figure 1: Frequency dependence of $\sigma_1(\omega)$ for the ruthenate $SrRuO_3$ at four temperatures. The different symbols represent the different experimental methods used in each frequency range, as explained in the text. The curves are the calculated values.

There are two main features of the high-frequency (infrared) data. First, $\sigma_1(\omega) \propto \omega^{-\alpha}$, with $\alpha = 0.4$, rather than the Drude value of $\alpha = 2$. Second, the $\sigma_1(\omega)$ data for different temperatures coalesce at high frequencies. Therefore, in the high-frequency regime, only the $\sigma_1(\omega)$ data at 40 K are displayed because these data are almost indistinguishable from those taken

at other temperatures.

2.2 High-temperature superconductors

Infrared $\sigma(\omega)$ data have been obtained by El Azrack *et al.* [3] and by Puchkov *et al.* [5] for the cuprates (high-T_c superconductors in the normal state). As was the case for $SrRuO_3$, the experimental results were found to be consistent with $\sigma_1(\omega) \propto \omega^{-\alpha}$, but with $\alpha \cong 0.7$. Thus, also for the cuprates, the Drude result ($\alpha = 2$) is not obtained. However, α has nearly twice the value that characterizes $SrRuO_3$.

The cuprate $YBa_2Cu_3O_{6.95}$ measured by Puchkov *et al.* [5] is an optimally-doped high-T_c superconductor and thus there is no pseudo-gap in the normal state to complicate the analysis. Moreover, the $\sigma_1(\omega)$ data we discuss here correspond to the electric field parallel to the a-axis and thus there is no contribution from the chains. Yet, even for this simplest case, Drude behavior was not found for $\sigma_1(\omega)$.

As was the case for the ruthenates, it was also found for $YBa_2Cu_3O_{6.95}$ in the normal state that the high-frequency $\sigma_1(\omega)$ data are almost independent of temperature [5].

3 Pippard ineffectiveness condition

3.1 Previous work

Many years ago, Pippard [7] pointed out that the finite mean free path of phonons in a metal requires a modification of the usual transport theory. He used this idea as the basis for a successful calculation of the seemingly anomalous ultrasonic attentuation of metals. Subsequently, Pippard's idea was extended by other workers to the finite mean free path of electrons, and has provided the explanation for a remarkable variety of transport data. These include the thermal conductivity [8] the reduction of the superconductor transition temperature of high-resistivity alloys [9] saturation effects in electron transport [10] the electrical resistivity of high-resistivity amorphous alloys [11, 12] the anomalous temperature dependence of the resistivity of potassium alloys [13] and negative deviations from Matthiessen's rule for irradiated samples of $SrRuO_3$ [14]. Here, we show that a generalization of Pippard's idea is also relevant to $\sigma_1(\omega)$ and can lead to non-Drude behavior.

3.2 Wave packets and ineffective electron scattering

A key feature in the analysis is that for materials having a high electrical resistivity, the electron mean free path is very short, and therefore, the electron can no longer be described as a wave with a sharp wave-vector value $\mathbf{k}$, but rather one has to deal with wave packets and a spread of $\mathbf{k}$-values [12]. As Cote and Meisels have explained (for electron-phonon scattering), the short electron mean free path implies that those phonons whose wavelength exceeds the electron mean free path are ineffective electron scatterers, and therefore the scattering is diminished [11, 12]. The Pippard condition is sometimes incorporated into the calculation of the electrical resistivity by removing the contribution of the low-$\mathbf{q}$ phonons from the resistivity integral [10].

For these reasons, when the Pippard idea is applied to electron transport, it is often referred to as the "Pippard ineffectiveness condition" [11]. This term implies that certain electron scattering processes are "ineffective" in degrading the current and thus do not contribute to the resistivity. As a result, the resistivity is smaller, or equivalently, the conductivity is *larger* than the value predicted without including the Pippard condition.

The Pippard idea also expresses itself in the $\sigma_1(\omega)$ data under discussion here. If $\sigma_1(\omega)$ is observed to fall off *more slowly* than quadratically with frequency ($\alpha \ll 2$), then the values of $\sigma_1(\omega)$ are *larger* than predicted by the Drude law, which does not take account of the Pippard ineffectiveness condition.

4 Discussion

4.1 Static electric fields

In the absence of scattering events, a static, spatially-independent electric field $\mathbf{E}$ drives a Bloch electron forward in $\mathbf{k}$-space according to the well-known equation

$$\hbar d\mathbf{k}/dt = -e\mathbf{E}. \tag{1}$$

It can be shown [15] using crystal-momentum representation that this equation is *exact* for Bloch electrons for a spatially-independent field $\mathbf{E}$.

There are two implications of electron scattering. First, one can no longer speak of a pure Bloch state having a specific quantum number $\mathbf{k}$, but one must speak of a wave packet centered around $\mathbf{k}$. Second, Eq. (1) for $d\mathbf{k}/dt$ is not exact, because the scattering potential (due to impurities, phonons,

etc.) is not spatially-independent. Therefore, the wave packet changes its shape somewhat as it moves in **k**-space under the influence of the field.

Since the shape of the wave packet changes, a single vector **k** is not sufficient to completely define the wave packet, implying an inherent ambiguity in the use of a vector **k** to describe an electron state. As a result, a scattering event is effective in degrading the current *only* if the electron wave packet is scattered to a final state *outside* the region of the ambiguity in **k**. Smaller-angle scattering events are *ineffective* (Pippard condition) and do not contribute to the resistivity because the electron wave packet does not "see" the scatterer [12].

4.2 Time-dependent electric fields

For time-dependent fields, there is an additional factor to be considered, namely, the effect on the resistivity of the oscillations of the electron wave packet. Such oscillations act to reduce the conductivity $\sigma_1(\omega)$, as given by the Drude law. However, the *effectiveness* of the frequency-dependent reduction of $\sigma_1(\omega)$ is mitigated by the fact that a single vector **k** is insufficient to completely describe the electron wave packet.

When a time-dependent electric field of frequency ω, $\mathbf{E} = \mathbf{E_o}e^{-i\omega t}$, is applied to a system of Bloch electrons, the change in the **k**-vector of the electrons, $\delta\mathbf{k}$, is given by

$$(d/dt)(\hbar\delta\mathbf{k}) = \hbar(\tau^{-1} - i\omega)\delta\mathbf{k} = -e\mathbf{E}. \tag{2}$$

Since the current $\mathbf{j}(= \sigma\mathbf{E})$ is given by $-ne\delta\mathbf{v} = (-ne\hbar/m)\delta\mathbf{k}$, where $\delta\mathbf{v}$ is the drift velocity, τ is the relaxation time, n is the electron density and m is an appropriate effective mass, it follows that

$$\sigma(\omega) = (ne^2/m)(\tau^{-1} - i\omega)^{-1}. \tag{3}$$

Equation (3) leads directly to the Drude law for $\sigma_1(\omega)$.

This standard derivation of the Drude law assumes that Eq. (2) for $\delta\mathbf{k}$ accurately describes the time dependence of the electron wave packet. However, because of electron scattering, Eq. (2) is not exact and the vector $\delta\mathbf{k}$ refers to the change in position in **k**-space of the wave packet, whose shape changes with time and hence *cannot* be described by a single vector **k**. Therefore, Eq. (3) is an approximation, which becomes increasingly poor as ω increases.

4.3 Qualitative discussion

It is useful to illustrate these ideas by means of a figure. The coefficient of $\hbar\delta\mathbf{k}$ in Eq. (2) can be considered a complex vector, which we denote by Ω (depicted in Fig. 2b), having real part τ^{-1} and imaginary part $-\omega$. Equation (3) may then be written $\sigma(\omega) = (ne^2/m)\Omega^{-1}$. The inverse complex vector Ω^{-1} has a magnitude that equals the reciprocal of the magnitude of Ω, and it is directed along the same angle α from the imaginary axis as is Ω but in the positive direction (Fig. 2a). The real part of Ω^{-1} gives the required quantity $\sigma_1(\omega)$.

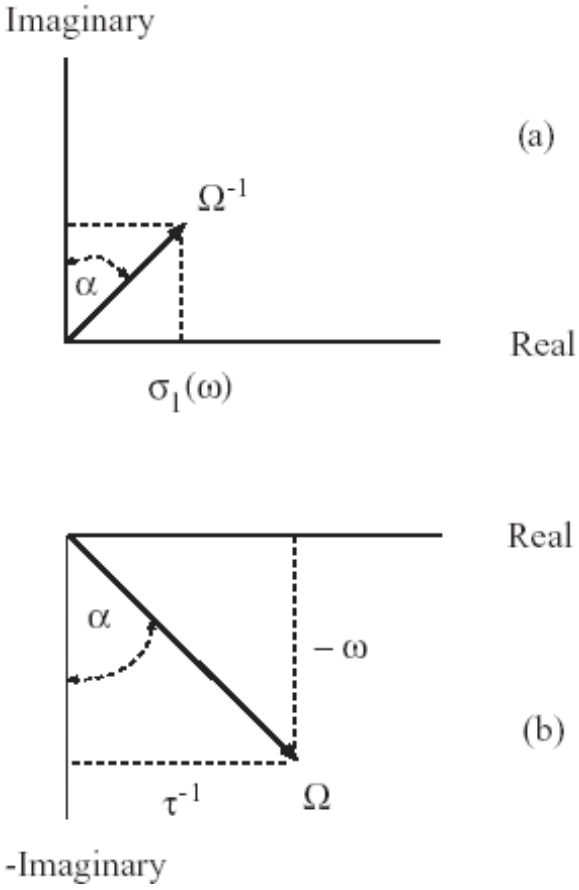

Figure 2: Schematic diagrams of the complex vectors (a) Ω^{-1} and (b) Ω. The angle α is the same for the two vectors.

As the frequency increases, the magnitude of the vector Ω increases and the angle α decreases as Ω rotates toward the imaginary axis. Accordingly, the vector Ω^{-1} also rotates toward the imaginary axis, since the angle α must be the same for both vectors. Moreover, its magnitude decreases. Consequently, at high frequencies, the real part of the vector Ω^{-1} is very small.

The Pippard ineffectiveness condition stems from the non-zero τ^{-1}, which leads to an ambiguity in $\mathbf{k}$. As a result, Eq. (2) is only an approximate expression for the dynamic behavior of the electron wave packet. This ambiguity in $\mathbf{k}$ (Eq. (2)) implies corresponding ambiguities in Ω and Ω^{-1} (Eq. (3)), and hence in $\sigma_1(\omega)$. At low frequencies for which $\sigma_1(\omega)$ is large, the approximate nature of Eq. (3) is unimportant. However, as the frequency increases, $\sigma_1(\omega)$ decreases until it becomes comparable in magnitude to its ambiguity. This retards the rate at which $\sigma_1(\omega)$ approaches zero. Thus, at sufficiently high frequencies, the Pippard condition must be included in the calculation of $\sigma_1(\omega)$.

For low-τ^{-1} materials (ordinary metals), the relevant frequencies are so high that the $\sigma_1(\omega)$ data are, in practice, unaffected by the Pippard condition. However, for the higher-τ^{-1} materials discussed here, the high-frequency regime will be seen to begin in the infrared region and the Pippard condition is therefore relevant to the data reported for $\sigma_1(\omega)$.

5 A simple model

A first-principles calculation of $\sigma_1(\omega)$ including the Pippard condition is beyond present capabilities. Therefore, we shall explore the consequences of a simple model which simulates the effect of the ambiguity in $\mathbf{k}$ on the frequency dependence of $\sigma_1(\omega)$. The key point to be modelled is that for high frequencies, $\sigma_1(\omega)$ becomes very small and is no longer accurately given by Eq. (3). The true value of $\sigma_1(\omega)$ is larger than predicted by Eq. (3), which does not include the Pippard condition.

In constructing the model, we turn for guidance to the static case of electron-phonon scattering. In that case, the Pippard *ineffectiveness* of small-$\mathbf{q}$ electron-phonon scattering is included in the calculation [9 - 14] by inserting into the resistivity integral, the "Pippard function" $f(q\lambda)$ (λ is the electron mean free path). This function, first derived by Pippard [7] is given by

$$f(y) = (2/\pi)[\frac{y\tan^{-1}(y)}{y - \tan^{-1}(y)} - \frac{3}{y}]. \tag{4}$$

As readily seen, the Pippard function approaches unity for a long electron mean free path and approaches zero as the mean free path diminishes. Because $f(q\lambda)$ is numerically almost undistinguishable from a phonon cutoff, in practice, a cutoff in the resistivity integral is often used in resistivity calculations [10 - 14].

Our model for the dynamic case consists of constructing a function analogous to the Pippard function for the static case. In the latter case, previous workers [10 - 15] have shown that the transport integrand derived without the Pippard condition is simply to be multiplied by the Pippard function. Similarly, in the dynamic case, the frequency in the expression for $\sigma_1(\omega)$ without the Pippard condition is to be divided by an appropriate function $F(\omega)$. The function $F(\omega)$ expresses the fact that at high frequencies, the oscillations are *ineffective* in reducing $\sigma_1(\omega)$ because the electron wave packet does not "feel" the rapid oscillations.

The basic idea is that the true frequency *with* the Pippard condition is equivalent to a smaller effective frequency *without* the Pippard condition. We thus include the Pippard condition by means of an effective frequency, that is, by replacing ω by $\omega/F(\omega)$, where the function $F(\omega)$ increases with increasing frequencies.

Since the magnitude of $\sigma_1(\omega)$ itself plays a central role in determining when the function $F(\omega)$ begins to deviate significantly from unity, $F(\omega)$ must depend on $\sigma_1(\omega)$, and we therefore write $F(\sigma_1(\omega))$. This leads to a kind of feedback effect, with $\sigma_1(\omega)$ influencing $F(\sigma_1(\omega))$, which in turn determines the value of $\sigma_1(\omega)$.

Expanding $F(\sigma_1(\omega))$ in a Taylor series and retaining only the first few terms yields,

$$F(\sigma_1(\omega)) \approx 1 + A_1/\sigma_1(\omega) + [A_2/\sigma_1(\omega)]^2 + [A_3/\sigma_1(\omega)]^3. \tag{5}$$

The values of the A_i depend in a complicated way on the material properties of the conductor under consideration. We take them to be adjustable parameters. In practice, we retained terms up to A_3, finding in each case that the A_3 term makes a negligible contribution for $F(\sigma_1(\omega))$. This justifies ignoring higher-order terms.

This completes the specification of the model. One obtains $\sigma_1(\omega)$ by writing the real part of Eq. (3) and replacing ω by $\omega/F(\sigma_1(\omega))$, which yields

$$\sigma_1(\omega) = (ne^2\tau/m)[1 + \omega^2\tau^2/F^2(\sigma_1(\omega))]^{-1}, \tag{6}$$

where $F(\sigma_1(\omega))$ is given by Eq. (5). The parameters A_i are chosen to give the best fit to the experimental data.

The proposed model has been specifically designed to simulate the consequences of the Pippard condition for $\sigma_1(\omega)$ and is not reliable beyond its intended purpose. In particular, the replacement of ω by $\omega/F(\sigma_1(\omega))$ is not an appropriate approximation for $\sigma_2(\omega)$, the imaginary part of $\sigma(\omega)$. Moreover, Eq. (6) does not accurately give $\sigma_1(\omega)$ for all frequencies, but only for the frequency range of the data. Therefore, it is not legitimate to extract values for $\sigma_2(\omega)$ from the values of $\sigma_1(\omega)$ given by Eq. (6) through the Kramers-Kronig relations.

6 Comparison with experiment

6.1 Low-resistivity materials

These materials include the ordinary metals and the conventional superconductors in the normal state. For these metals, the electrical resistivity is 1-2 orders of magnitude smaller than for the ruthenates and the cuprates in the normal state. As a result, the first term in (5) dominates, yielding $F(\sigma_1(\omega)) \approx 1$. Hence, one immediately recovers the Drude law. Because the ambiguity in **k**-space is very small for low-resistivity materials, the Pippard condition is correspondingly inconsequential.

	$SrRuO_3$	$YBa_2Cu_3O_{6.95}$	$Bi_2Sr_2CaCu_2O_8$	$Bi_2Sr_2Ca_2Cu_3O_{10}$
$A_1/\sigma_1(\omega)$	60	1.45	28	16
$[A_2/\sigma_1(\omega)]^2$	141	0.02	-	-
$[A_3/\sigma_1(\omega)]^3$	0.0	0.00	-	-

Table 1: Values of the ratios $[A_i/\sigma_1(\omega)]^i$ at a frequency in the infrared regime ($\omega = 1000$ cm^{-1}). The values were obtained by fitting to the $\sigma_1(\omega)$ data for the ruthenate $SrRuO_3$ and for the high-temperature superconductors in the normal state, as discussed in the text ($YBa_2Cu_3O_{6.95}$, $Bi_2Sr_2CaCu_2O_8$ and $Bi_2Sr_2Ca_2Cu_3O_{10}$).

6.2 High-resistivity materials - ruthenates

For the ruthenates, the resistivity is so high that the function $F(\sigma_1(\omega))$ plays a significant role. Therefore, the Pippard condition is important. Solving Eq. (6) for $\sigma_1(\omega)$ as a function of ω yields the curves in Fig. 1 for the four measured temperatures. One notes the agreement between the curves and the experimental points. Therefore, the model does seem to have some relevance to the $\sigma_1(\omega)$ data.

In Table 1, we present the values obtained for the three ratios $[A_i/\sigma_1(\omega)]^i$ at an infrared frequency ($\omega = 1000$ cm^{-1}). It is seen that $[A_3/\sigma_1(\omega)]^3$ is negligible.

What is presented here cannot be the whole story. The function $F(\sigma_1(\omega))$ was approximated by a Taylor expansion. Moreover, at sufficiently high frequencies, the model must break down and one returns to the Drude limit for $\sigma_1(\omega)$ to ensure that the Fourier transform of the response function does not correspond to an infinite perturbation at time zero. In practice, however, interband transitions prevent this high-frequency limit from being realized.

Examining the resulting values of the parameters A_i shows that the term containing A_2 is dominant. If one discards the other terms, a straightforward analysis of Eq. (6) yields that at high frequencies, $\sigma_1(\omega) \propto \omega^{-2/5}$, as reported [1] for these data. Moreover, the curves for $\sigma_1(\omega)$ coalesce at high frequencies, independent of the temperature (relaxation time), which is also consistent with the data.

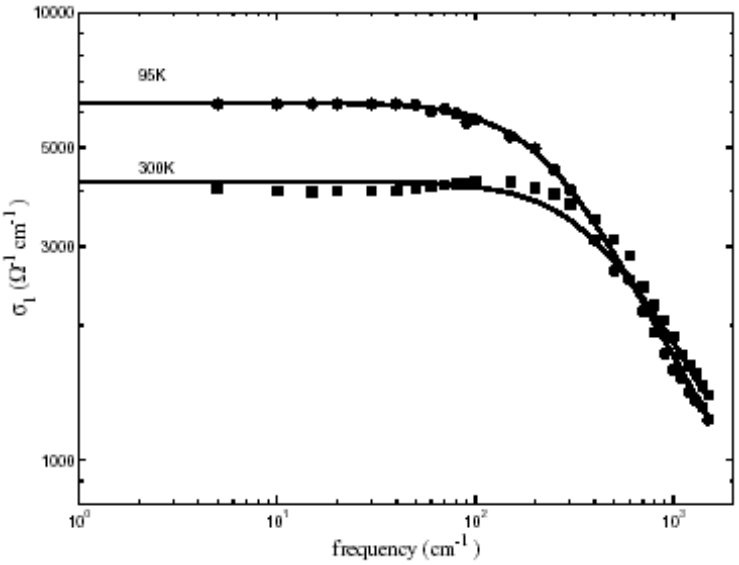

Figure 3: Frequency dependence of $\sigma_1(\omega)$ for the cuprate superconductor $YBa_2Cu_3O_{6.95}$ measured at two temperatures above T_c. The curves are the calculated values.

6.3 High-resistivity materials - cuprates

In Fig. 3, we display the $\sigma_1(\omega)$ data for the optimally doped cuprate superconductor $YBa_2Cu_3O_{6.95}$ measured by Puchkov *et al.* [5] at two different temperatures above T_c. The curves in Fig. 3 represent the solutions to Eq. (6) for $\sigma_1(\omega)$ at the measured temperatures.

In Table 1, we present the values obtained for the three ratios $[A_i/\sigma_1(\omega)]^i$ at a frequency in the infrared regime ($\omega = 1000$ cm^{-1}).

It is seen from Table 1 that the dominant term is $A_1/\sigma_1(\omega)$. If one discards the other A_i terms, analysis of Eq. (6) yields that at high frequencies, $\sigma_1(\omega) \propto \omega^{-2/3}$, in agreement with the data. Moreover, the curves for $\sigma_1(\omega)$ tend to coalesce at high frequencies, independent of the temperature (relaxation time), which is also consistent with the data.

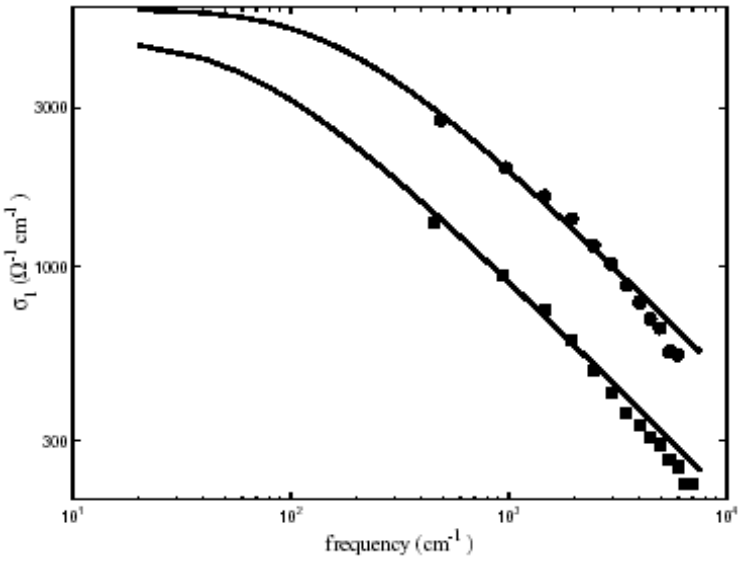

Figure 4: Frequency dependence of $\sigma_1(\omega)$ for cuprate superconductors measured at room temperature. The upper and lower symbols represent $Bi_2Sr_2CaCu_2O_8$ and $Bi_2Sr_2Ca_2Cu_3O_{10}$, respectively. The curves are the calculated values.

Measurements of $\sigma_1(\omega)$ have also been carried out at room temperature for a number of cuprate superconductors by El Azrak *et al.* [3] In all cases, $\sigma_1(\omega)$ exhibits power-law behavior at high frequencies, $\sigma_1(\omega) \propto \omega^{-\alpha}$, with the observed value [16] of the exponent being $\alpha \cong 0.7$. We shall focus on

$Bi_2Sr_2CaCu_2O_8$ and $Bi_2Sr_2Ca_2Cu_3O_{10}$ because the $\sigma_1(\omega)$ data for these two superconductors had the least scatter.

The experimental values for $\sigma_1(\omega)$ for $Bi_2Sr_2Ca_2Cu_3O_{10}$ and $Bi_2Sr_2CaCu_2O_8$ are presented in Fig. 4. Since each superconductor was measured only at a single temperature (room temperature), there are insufficient data to determine all of the A_i parameters. Therefore, we build on the results obtained for the other cuprate, and assume that the A_1 term is dominant. This yields the curves in Fig. 4. In particular, $\sigma_1(\omega) \propto \omega^{-2/3}$ at high frequencies, in agreement with the data.

7 Summary and conclusions

We have shown that for very-high-resistivity materials, the Pippard ineffectiveness condition may play an important role in the analysis of $\sigma_1(\omega)$ and may lead to significant deviations from the Drude law. We have applied our results for $\sigma_1(\omega)$ to the ruthenates and to the cuprate superconductors in the normal state, finding agreement with experiment for each material. This does not, of course, prove that the Pippard condition is the correct explanation for the non-Drude behavior observed for $\sigma_1(\omega)$ for these materials. However, our results do indicate that for high-resistivity materials, non-Drude behavior for $\sigma_1(\omega)$ cannot be taken as evidence for anomalous behavior which cannot be explained within the framework of the Landau fermi-liquid theory.

L.K. acknowledges support by the Israel Science Foundation founded by the Israel Academy of Sciences and Humanities.

References

[1] J.S. Dodge, C.P. Weber, J. Corson, J. Orenstein, Z. Schlesinger, J.W. Reiner, and M.R. Beasley, Phys. Rev. Lett. **85**, 4932 (2000).

[2] P. Kostic Y. Okada, N.C. Collins, Z. Schlesinger, J.W. Reiner, L. Klein, A. Kapitulnik, T.H. Geballe, and M.R. Beasley, Phys. Rev. Lett. **81**, 2498 (1998).

[3] A. El Azrak, R. Nahoum, N. Bontemps, M. GuillouxViry, C. Thivet, A. Perrin, S. Labdi, Z.Z. Li, and H. Raffy, Phys. Rev. B **49**, 9846 (1994).

[4] Z. Schlesinger, R.T. Collins, F. Holtzberg, C. Feild, S.H. Blanton, U. Welp, G.W. Crabtree, Y. Fang, and J.Z. Liu, Phys. Rev. Lett. **65**, 801 (1990).

[5] A.V. Puchkov, D.N. Basov, and T. Timusk, J. Phys.: Condens. Matt. **8**, 10049 (1996), see Fig. 8.

[6] G. Santi and T. Jarlborg, J. Phys.: Condens. Matt. **9**, 9563 (1997).

[7] A.B. Pippard, Philos. Mag. **46**, 1104 (1955).

[8] J.E. Zimmerman, J. Phys. Chem. Solids **11**, 299 (1959).

[9] L.V. Meisels and P.J. Cote, Phys. Rev. B **19**, 4514 (1979).

[10] P.J. Cote and L.V. Meisels, Phys. Rev. Lett. **40**, 1586 (1978).

[11] L.V. Meisels and P.J. Cote, Phys. Rev. B **30**, 1743 (1984).

[12] J. Laakkonen and R.M. Nieminen, Phys. Rev. B **34**, 567 (1986).

[13] N. Wiser, J. Phys. F **18**, 457 (1988); M. Kaveh and N. Wiser, Phys. Rev. B **36**, 6339 (1987).

[14] L. Klein, Y. Kats, N. Wiser, M. Konczykowski, J.W. Reiner, T.H. Geballe, M.R. Beasley, and A. Kapitulnik, Europhys. Lett. **55**, 532 (2001).

[15] L.D. Landau and E.M. Lifshitz, *Quantum Mechanics*, transl. J.B. Sykes and J.S. Bell (Pergamon Press, London and New York, 1958), pp. 389-394.

[16] See Ref. 3, Fig. 8 and Table II.